CHAPTER-4

Study of bioactivity of V_2O_5 substituted

1393-B3 Borate glass

4.1 Introduction

Since other metals like steel and iron have different mechanical and structural characteristics, bioactive glass is a material substitute for bone. Human healing has evolved thanks to medical knowledge. Can it reverse irreversible deterioration and damage? Scientists are creating new materials to fulfil that requirement on behalf of our bodies. It is excellent to replace such body parts using bioceramic materials [1]. Calcium is a common component of bioactive glass, and it combines with blood phosphorus to generate hydroxyapatite (HA). Bone is made of an inorganic substance [2]. Bioactive glasses are utilized to generate desired structures instead of bone. As a result, we are creating new bioactive materials and evaluating how well they work with biological tissues. SiO_2 is the primary use for B_2O_3 and borate glasses, but they are being thoroughly studied [3]. Glass formation is most likely to occur when B_2O_3 is molten since it cannot crystallize when cooled gradually. Following the complete substitution of B_2O_3 for SiO_2, 1393-B3 bioglass was created [4]. Bioglasses based on borate break down more quickly than glasses based on silicate, which produce HA more quickly [5]. While borate glasses have a higher SiO_2 layer than apatite-like silicate bioglasses, SBF does not [6]. 1393B3 Because bioactive glasses are both biocompatible and active, they are frequently used and doped with different substances. To create an HA layer for bone regeneration modelling, borate glass reacts with biological fluids to produce functional ions that mineralize and alkalinize samples. We replace 1393-B3 borate glass with transition material V_2O_5. Amphoteric vanadium oxide (V_2O_5) exhibits both basic and acidic properties. These changes get oxidized by V_2O_5. Better for orthopaedics and tissue compatibility, borosilicate glass contains V_2O_5 [7]. Human tissues suffer from vanadium (V) oxide. Up to 2.5%, smaller amounts were utilized.

4.2 Experimental details:

The 1393-B3 bioactive glass with composition (53-x) B_2O_3-xV_2O_5-6Na_2O-20CaO-4P_2O_5-12K_2O-5MgO (x=0, 1, 1.5, 2 and 2.5 wt%) was prepared using a solid-state method

having composition shown in table 4.1. In an electric furnace, the weighted mixture was melted in a platinum crucible at 1100°C for two hours at a rate of 4°C per minute. The molten sample was shaped into a steel frame, annealed at 500°C for an hour, and then cooled at 1°C per minute in the furnace. Crushing the final product with a 10:1 zirconia ball-to-powder ratio until the particles are smaller than 38μm.

Table 4.1 Bioactive V_2O_5 substituted 1393-B3 glass compositions (wt %)

Sample Code	**B_2O_3**	**Na_2O**	**K_2O**	**CaO**	**MgO**	**P_2O_5**	**V_2O_5**
Base	53	6	12	20	5	4	0
Vb1	52	6	12	20	5	4	1
Vb2	51.5	6	12	20	5	4	1.5
Vb3	51	6	12	20	5	4	2
Vb4	50.5	6	12	20	5	4	2.5

4.2.1 *In-vitro* Bioactivity:

Kokubo et al. [8] used a well-known technique to prepare SBF. Powdered samples were immersed in SBF solution at 37 °C for 2, 7, 10, 15, 21, and 28 days in order to investigate this. Using an EI Alpha 01 Digital pH Meter, we determined the pH of 1393-B3 bioactive glass samples that had been soaked in SBF at room temperature. After that, they were dried for 48 hours at 70°C in an oven. The JASCO FTIR 4600 (FTIR) instrument was utilized to assess the variation in bond formation before and after SBF immersion within the range of 450-3500 cm-1. The crystalline structure of the samples was examined using the Rigaku Miniflex 600 Desktop X-Ray Diffraction (XRD) instrument both before and after the samples were immersed in SBF for 15 and 28 days. Sample morphology was assessed before and after 15,

28, and 16 days of SBF immersion using the SEM instrument EVO (Scanning Electron Microscope MA15 / 18).

4.2.2 Hemocompatibility:

The human blood sample was taken in tubes coated with the anticoagulant heparin to assess hemocompatibility. Next, the tubes were turned. The liquid above the sediment, known as the supernatant, was carefully cleaned and disposed of. After washing the RBC pellets with cold PBS (Phosphate-Buffered-Saline), blood and PBS were mixed at a ratio of 1:10. We mixed 0.9 ml of 1 mg/ml products in PBS with 0.1 ml of RBC solution. Triton x-100 was positive (100 lysis), while base PBS (pH 7.4) was negative (no lysis). To separate the mixture from non-lysed RBCs, centrifuge it at 650 g for 10 minutes at 4ºC after incubating it at 37 ± 1 °C for an hour while stirring continuously. Using a microplate reader, the blood lysis was measured by supernatant optical density at 540 nm.

$$\boldsymbol{Hemolysis = \frac{ODsample - OD0}{OD100 - OD0} X\ 100}$$

Where ODsample,OD0,OD100 are the optical density of the samples, negative and positive control.

4.2.3 Biological Characterization:

The maintenance of MG-63 cell lines was investigated in a CO_2-humidified incubator at 37°C. Dulbecco's Modified Eagle Medium (DMEM) was used to culture the cells, and FBS (fetal bovine serum) was added as a supplement. Microbiologically, sterile penicillin-streptomycin cultures were uncontaminated. Nutrient-rich, healthy environments promote the growth and multiplication of MG-63 cells. We used MTT to investigate the effects of prepared glass samples on the proliferation of MG-63 cells. Ten thousand cells were allowed to bond together overnight in each 96-well cell growth plate. One millilitre of 5 mg/ml PBS was added

to the prepared glass samples. MTT-containing media was added to each well and removed after the cells were exposed to varying doses (100µg/ml, 200µg/ml, 400µg/ml, and 600µg/ml) at a constant temperature for 24 hours. After two hours of incubation, 100 µl of DMSO was added to each well, replacing the MTT-containing solution. We left the wells incubated for a further half hour. Absorbance at 570 nm was measured by multiplate readers. Phase contrast lenses showed the proliferation of the MG-63 cell line. In each well of a 12-well tissue culture plate, we cultivated 1 x 105 MDA-MB-231 cells for 24 hours at 37°C in humidified air with 5% CO_2. Samples that were ready were given to the cells. Images from a 100x inverted phase contrast microscope (EVOS FL cell imaging instrument, Life Technologies, USA) were acquired following a 24-hour course of therapy.

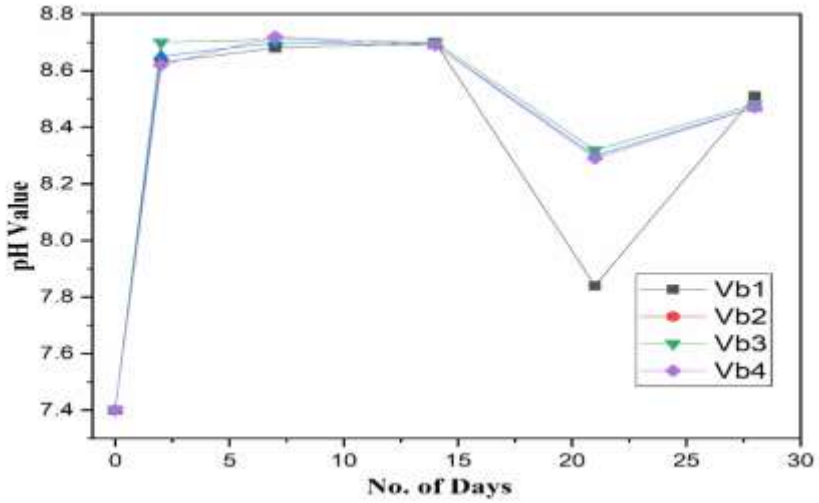

Figure 4.1 pH variation of prepared samples

4.3. Result and Discussion:

4.3.1 *In-vitro* analysis:

After SBF immersion, the pH of the bioglass samples increases (Figure 4.1). As HA layers formed, ion exchange between oxygen atoms and alkali ions (Na+, etc.) in glass samples. When chemical reactions stabilize, ion exchange ceases. Bioactivity is determined using data on HA formation stability.

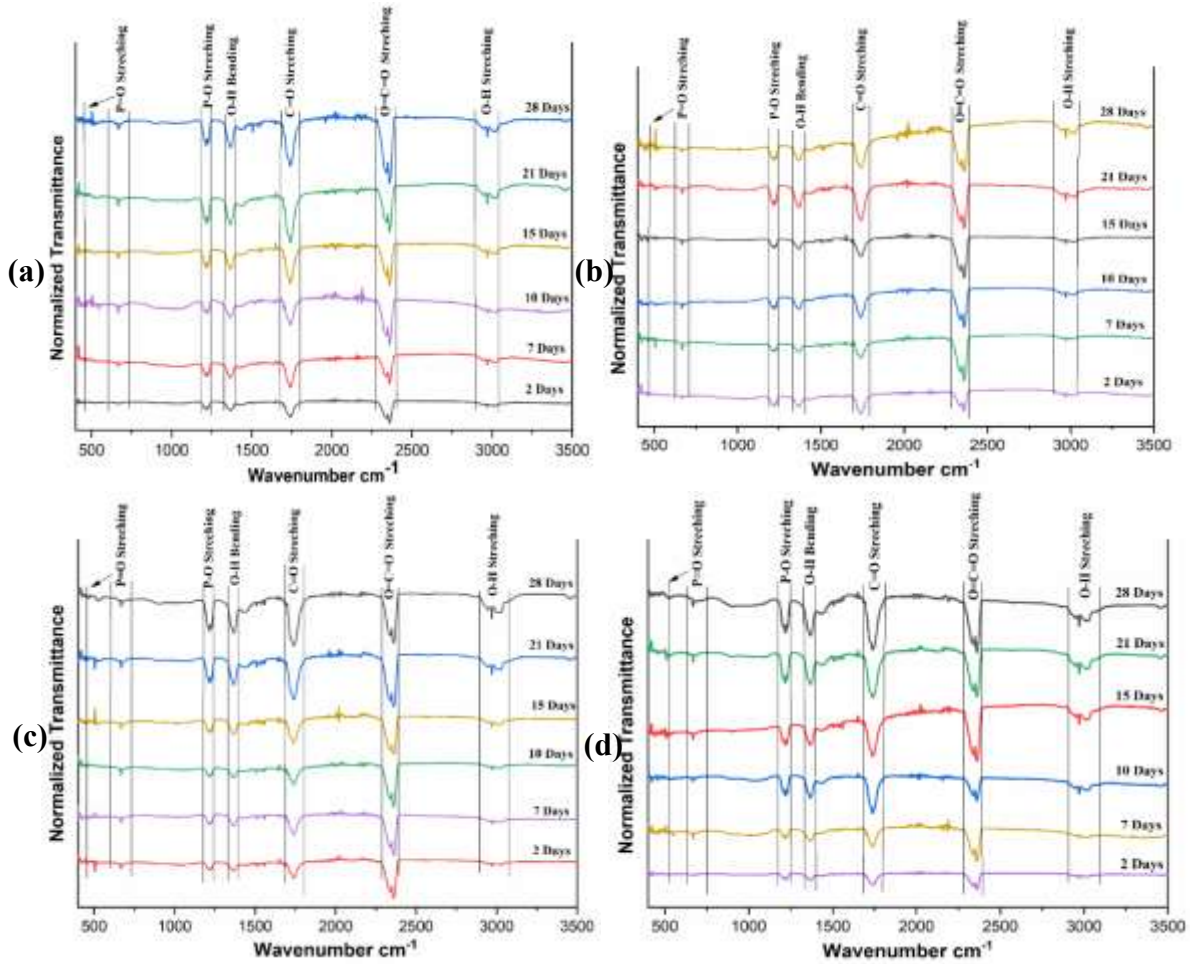

Figure 4.2 FTIR graph for **(a)** Vb1 **(b)** Vb2 **(c)** Vb3 **(d)** Vb4 samples for corresponding SBF immersion days

The FTIR transmittance spectroscopy study of the bioglass samples was utilized to investigate the functional group. The functional group present in Vb1, Vb2, Vb3, and Vb4 for various time intervals, as well as various SBF immersion times, is depicted in Fig. 4.2 (a-d). The functional groups 470 cm-1, 620-720 cm-1 (P=O bond), and 1185-1245 cm-1 (P-O bond) stretch here indicate the phosphate bond formation. The FTIR reveals the production of hydroxyl bonds at 1320 cm-1 to 1410 cm-1 (O-H bending) and 2890-3050 cm−1 (O-H stretching). Furthermore, carbonyl bonds are represented by the peak ranges of 1690–1790 cm−1 (C=O stretching) and 2290–2390 cm−1 (O=C=O stretching) [9]. These weren't there in the early phases, as the corresponding graphs demonstrate. The creation of HA bonds in the corresponding samples following their immersion in the SBF is what led to these positive

results. After samples are soaked in SBF solution for 28 days, bond peaks become more pronounced. Thus, it causes the samples in question to become more bioactive.

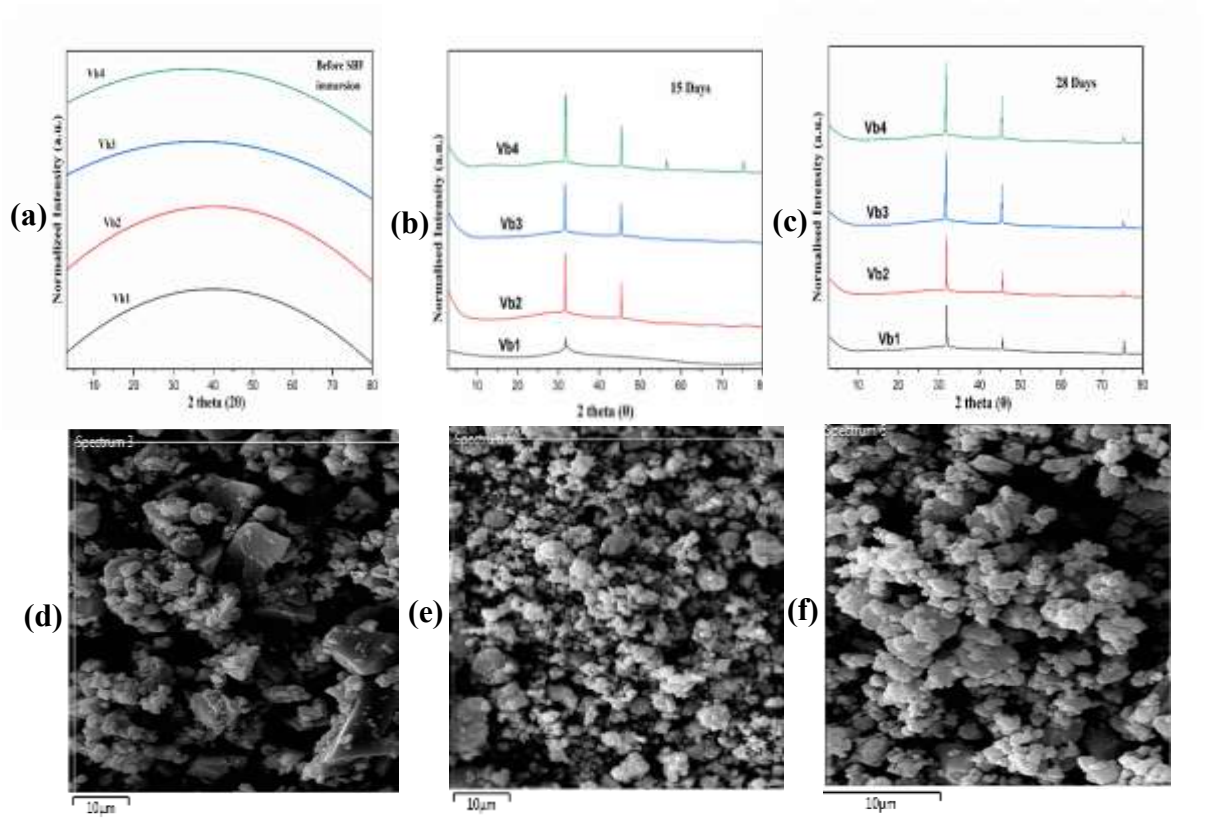

Figure 4.3 XRD graph for V_2O_5 substituted 1393-B3 glass **(a)** before SBF and after SBF immersion for **(b)** 15 days **(c)** 28 days, SBF images for the samples **(d)** before SBF and SBF immersion for **(e)** 15 days **(f)** 28 days.

Phase analysis reveals that the 1393-B3 glass samples, both with and without V_2O_5 substitution, are amorphous and lack a crystalline phase. Before SBF immersion, none of the produced samples in Figure 4.3a XRD showed a strong peak. However, after V_2O_5 replacement, two large peaks were found in the glass samples 1393-B3 (Figure 4.3b-c). At 31.7º (2θ), a prominent peak indicates the presence of $Ca_{10.042}(PO_4)_{5.952}(OH)_{2.292}$ (JCPDS code-2536). While V_2O_5-substituted samples immersed in SBF solution for 15 and 28 days form HA bonds, JCPDS data shows HA bonds in the borate base. HA growth is seen in SEM micrographs after SBF immersion in V_2O_5. 2.5% V_2O_5 substituted 1393-B3 glasses are shown in Figure (4.3d) without any white deposition prior to SBF. The sample surfaces displayed in Figure (4.3e–f) exhibit white areas where the HA layer has formed after 15 and 28 days of SBF immersion.

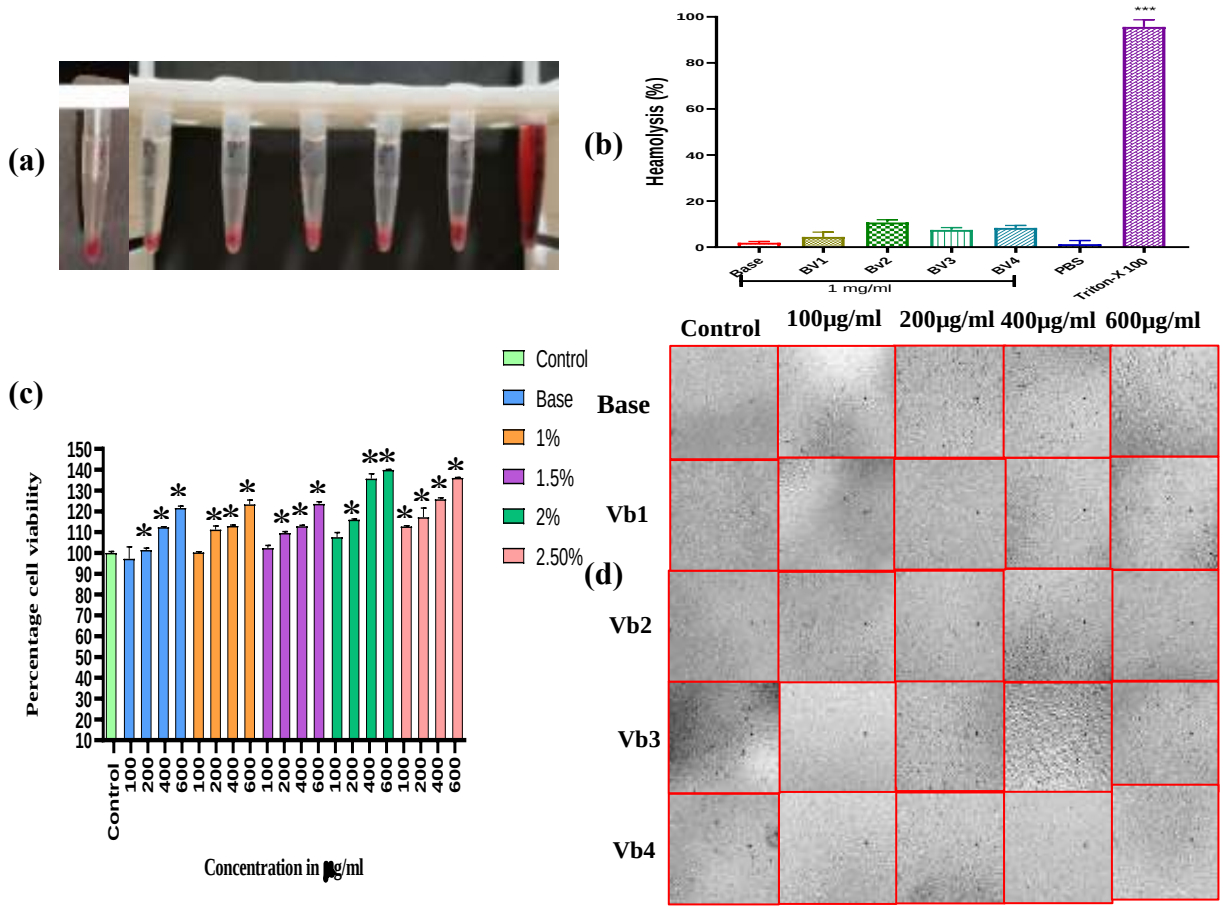

Figure 4.4 Ex vivo Hemocompatibility and cellular compatibility of the developed product; **(a)** represents the after hemolytic study, **(b)** % of hemolytic activity **(c) %** Cellular viability **(d)** Phase contrast image for variable concentration.

4.3.2 Hemocompatibility:

Based on the results, all of the samples were compatible with human blood (Figure 4.4.a) because there was no blood sample lysis. As compared to the positive control group (triton x-100) in Figure 4.4.b, the products displayed less than 4% hemolysis, which was significantly lower ($p < 0.01$) [11]. Thus, the generated samples were deemed suitable for orthopaedic use and compatible with blood.

4.3.3 In Vitro Cellular Analysis:

We found that all of the samples we obtained following V_2O_5 substitution are biocompatible, as evidenced by the phase contrast images and bar graph presented in this study (Figure 4.4.c). The cellular proliferation of substituted V_2O_5 improves and remains steady with increasing substitution.

V_2O_5-substituted 1393-B3 borate glass samples (Base, 1%-2.5%) exhibited concentration-dependent proliferation against MG-63 cells, even at higher concentrations, according to a cellular compatibility analysis. Proliferation was higher in the treatment group compared to the control group. Tukey's test and one-way ANOVA were employed in the statistical analysis. * Denotes a significant variation (proliferation) when compared to the control group at $p<0.05$.

As seen in Figure 4.4.d, cells are helped to survive and proliferate in V_2O_5-substituted 1393-B3 borate glass, indicating the possibility of bone repair. The pictures demonstrate how MG-63 cell growth was enhanced by V_2O_5-substituted 1393-B3 glass samples. This validates the test for cellular compatibility.

4.4 Summary:

To conclude, a solid-state method was used to create a base, and V_2O_5 substituted 1393-B3 bioactive glasses. The bioactivity of the base and V_2O_5 substituted 1393-B3 borate glass was shown by FTIR to increase with longer SBF soaking times. HA bonds were highest in samples that were immersed in SBF for 28 days. XRD data indicates that the produced samples were amorphous at first. Nonetheless, following 15 and 28 days of SBF soaking, HA peaks were seen. After SBF immersion for 15 and 28 days, SEM micrographs over prepared samples demonstrate the formation of the HA layer. Its compatibility with human blood is demonstrated by hemocompatibility. Cellular compatibility and phase contrast images show improved biocompatibility with the MG-63 osteosarcoma cell line following V_2O_5 substitution in 1393-B3 glass samples. The present study assessed the effects of 1393-B3 borate bioglass on V_2O_5 partial B_2O_3 replacement (1% to 2.5%), which has a major bearing on orthopaedic implants applications used in bone healing.

References

[1] L.L. Hench, The story of Bioglass®, Journal of Materials Science: Materials in Medicine, 17 (2006) 967-978.

[2] P. Ducheyne, Q. Qiu, Bioactive ceramics: the effect of surface reactivity on bone formation and bone cell function, Biomaterials, 20 (1999) 2287–2303.

[3] S. Yamaguchi, Borate bioactive glass, Bioactive Glasses and Glass-Ceramics: Fundamentals and Applications, 5 (2022) 79-86.

[4] A.M. Deliormanlı, Synthesis and characterization of cerium- and gallium-containing borate bioactive glass scaffolds for bone tissue engineering, Journal of Materials Science: Material in Medicine 26 (2015) 1573-4838.

[5] Q. Fu, M.N. Rahaman, H. Fu, X. Liu, Silicate, borosilicate, and borate bioactive glass scaffolds with controllable degradation rate for bone tissue engineering applications. I. Preparation and in vitro degradation, Journal of biomedical materials research. Part A, 95 (2010) 164-171.

[6] A. Yao, D. Wang, W. Huang, Q. Fu, M.N. Rahaman, D.E. Day, In vitro bioactive characteristics of borate-based glasses with controllable degradation behavior, Journal of the American Ceramic Society, 90 (2007) 303-306.

[7] A. Singh, P. Goswami, B. Koch, P. Singh, R. Pyare, Study of Human Osteosarcoma Cell Line Growth, Hemocompatibility, In-vitro Analysis and Physical Properties of V_2O_5 Substituted Borosilicate Glass, Silicon (2024) 1876-9918.

[8] T. Kokubo, H. Kushitani, S. Sakka, T. Kitsugi, T. Yamamuro, Solutions able to reproduce in vivo surface-structure changes in bioactive glass-ceramic A-W3. Journal of Biomedical Materials Research, 24 (1990) 721–734.

[9] J. Xia, Y. Xiong, S. Min, J. Li, A review of recent infrared spectroscopy research for paper, Applied Spectroscopy Reviews 58 (2022) 738-754.

[10] S. Yadav, P. Singh, R. Pyare, Synthesis, characterization, mechanical and biological properties of biocomposite based on zirconia containing 1393 bioactive glass with hydroxyapatite, Ceramics International 46 (2020) 10442–10451.

[11] A. Ali, M. Ershad, V. K. Vyas, S. K. Hira, P. P. Manna, B. N. Singh, S. Yadav, P. Srivastava, S. P. Singh, R. Pyare, Studies on effect of CuO addition on mechanical properties and in vitro cytocompatibility in 1393 bioactive glass scaffold, Materials Science and Engineering: C 93 (2018) 341–355.